JMS2A: Joint Multi-source Domain and Two-step Alignment Strategy for Cross-subject EEG Emotion Recognition

Yang Tian (yang_tian@stu.xidian.edu.cn)
Liying Yang* (yangliying1208@163.com)
Jingtao Du (jtdu@stu.xidian.edu.cn)
Huanyu He (23031212455@stu.xidian.edu.cn)
Department of Computer Science and
Technology, Xidian University, Xi'an, China

Abstract

Emotion recognition based on electroencephalography (EEG) plays a significant role in brain-computer interface (BCI) applications. However, individual differences often hinder the generalization of emotion recognition methods to unknown subjects. To address this, we propose an unsupervised domain adaptive model with joint multi-source domain and two-step alignment strategy (JMS2A). The alignment strategy consists of two steps: (1) To capture the structured information from source domain, we combine multiple source domains into a mixed source domain. Simultaneously, a single source domain and the target domain are combined to form a pseudo-target domain, which is then indirectly aligned with the mixed source domain; (2) To extract latent class information from the target domain, we extend supervised contrastive learning to enable direct alignment between source and target domain. We evaluated JMS2A on the SEED and SEED-IV datasets, achieving accuracies of 95.30% and 86.55%, respectively. Experimental results demonstrate that our approach outperforms state-of-the-art methods. The source code is available at https://github.com/cccyangt/JMS2A.

Keywords: EEG; emotion recognition; Multi-source domain; Transfer learning

Introduction

Emotion is a physiological activity in humans that significantly influences our cognitive processes, especially in areas such as learning, decision-making, and memory (Tyng et al., 2017). Human facial expressions and body movements cannot accurately reflect true emotions, as they are often deliberately masked (Ekman, 1993). The brain, as a central part of the nervous system, controls and regulates emotions, making it effective and reliable to use electroencephalographic (EEG) signals that reflect brain activity for recognizing an individual's current emotional state (Paranjape et al., 2001).

In recent years, significant progress has been made in emotion recognition using EEG signals. However, most of these studies are subject-dependent, assuming that the data in the training and testing sets are independently and identically distributed. Consequently, these methods typically perform poorly when tested on new individuals due to differences in EEG signals between subjects, which violate the independent and identically distributed assumption. Additionally, EEG signals are highly non-stationary (Lotte et al., 2018). To address these issues, researchers have introduced unsupervised domain adaptation (UDA) methods into EEG-based emotion recognition, utilizing labeled data from one individual to classify data from new individuals, allowing existing emotion recognition models to be applied to unknown subjects (Saha et al., 2019).

With the rapid development of neural networks, unsupervised domain adaptation based on deep learning has attracted attention because it can end-to-end extract transferable features across subjects (M. Wang & Deng, 2018). Jin et al. (2017) introduced Domain-Adversarial Neural Networks (DANN) into cross-subject emotion recognition, where DANN constructs a domain discriminator through a gradient reversal layer to minimize domain discrepancies, thereby improving cross-subject emotion recognition performance. Y. Li et al. (2018), inspired by neuroscience, focused on the asymmetry of emotional responses between the left and right hemispheres of the brain, proposing the Bi-Domain Adversarial Neural Network (BiDANN) model. This model designs a global domain and two local domain discriminators to learn discriminative features related to emotional perception from each brain hemisphere, improving feature stability across different domain shifts. X. Li et al. (2024) proposed a graph-based unsupervised sub-domain adaptation (Gusa) method, which performs fine-grained alignment between source and target domains from both channel and emotional sub-domains. Meanwhile, attention mechanisms have been employed to enhance cross-subject emotion recognition performance. Xu et al. (2023) proposed the Attention-based Multi-dimensional EEG Transformation (AMDET) model, which leverages a multi-dimensional global attention mechanism to exploit the complementary nature of frequency-space-time features in EEG data for effective feature extraction.

The above methods merge all subjects into a single source domain. This simple merging improves the model's performance by expanding the training data. However, it overlooks the differences between subjects, making it difficult to align multiple different distributions simultaneously, which limits the model's performance in feature extraction. Therefore, multi-source domain adaptation has emerged as a practical solution.

In multi-source domain adaptation, multiple labeled source domains and a single unlabeled target domain are aligned to extract domain-invariant features through fine-grained structure learning for each source and target domain. Researchers have made significant progress in the field of EEG-based emotion recognition by utilizing multi-source domain adaptation. For example, F. Wang et al. (2021) constructed a dedicated classifier for each source domain and used multi-kernel maximum mean discrepancy to optimize the classi-

In D. Barner, N.R. Bramley, A. Ruggeri and C.M. Walker (Eds.), *Proceedings of the 47th Annual Conference of the Cognitive Science Society*

fiers in an attempt to explore domain-invariant structures. Although the model's performance was reasonable, this study used labels from the target domain, which are inaccessible in unsupervised domain adaptation. To overcome this, Chen et al. (2021) extended prior work by considering both domain-invariance and domain-specificity in EEG emotion recognition. They constructed a dedicated feature extractor for each source domain to extract domain-specific features, enabling finer-grained domain alignment. Y. Yang et al. (2024) introduced attentional alignment methods in multi-source domain adaptation, utilizing the domain attention mechanism and domain consistency loss in learning and aligning rich domain invariant features. However, these works assume inter-class separation in EEG data and therefore only consider alignment between different domains while ignoring the finer-grained alignment of classes between different domains. Additionally, they overlook exploring structured information in source domain data and latent class information in target domain data, which may result in suboptimal performance.

In order to overcome these limitations, we propose JMS2A, an unsupervised domain adaptive model with joint multi-source domain and two-step alignment strategy. The model consists of three modules and a two-step alignment strategy. First, we construct a common feature extractor to extract shallow common features from both source and target domains while executing the first step of the alignment strategy, indirectly aligning the common features. Since each subject's features have their own specificity, we input them into domain-specific feature extractors to extract deep differential features, and then perform a two-step alignment strategy. In the second step, the differential features are directly aligned. Finally, we train a classifier for each source domain, and the model's output is averaged from the predictions of all classifiers.

The main contributions of this paper are summarized as follows:

(1)We propose JMS2A, an unsupervised domain adaptive model with joint multi-source domain and two-step alignment strategy. The common and differential features extracted by the model solve the problem of domain alignment in shallow and deep feature spaces, which is ignored by other methods.

(2) We design a two-step alignment strategy that mines the structured information of the source domain data as well as extracts the potential class information of the target domain data, resulting in a model with better performance.

(3) The experimental results demonstrate that our model outperforms others in cross-subject classification tasks.

Methodology

In this section, we provide an overview of the JMS2A model's overall structure, which consists of three components: (1) a common feature extractor, (2) domain-specific feature extractors, and (3) domain-specific classifiers. We then focus on the two-step alignment strategy employed by the JMS2A model, which is divided into two stages: (1) indirect alignment of shallow common features and (2) direct alignment of deep distinctive features.

Model Structure

As shown in Figure 1, the input to the JMS2A model consists of n independent source domain data, corresponding target domain data, and a mixed source domain formed by combining the n independent source domains. These inputs are passed through the common feature extractor to obtain the shallow common features. The shallow features are then fed into the corresponding domain-specific feature extractors to obtain the deep distinctive features. Based on the shallow and deep features, the two-step alignment strategy is performed. The resulting deep features are then passed into the domain-specific classifiers to obtain the corresponding classification predictions. The classification loss is computed based on the predictions from the source domains. Finally, the model output is the average of the predicted values from all classifiers. The details of each module are as follows.

Feature Extractor The common feature extractor maps the source and target domain data from the original feature space to the shallow common feature space. These shallow features capture the commonality between the source and target domain data and represent domain-invariant information. On the other hand, the domain-specific feature extractors map the source and target domain data to deep, unique feature spaces. These deep features represent the differences between the data. Notably, batch normalization layers (Ioffe, 2015) are introduced after each hidden layer to standardize the data and obtain more robust feature representations. Specifically, the feature extractor can be constructed by stacking the following formulas:

$$Z = \text{Dropout}(\text{ReLU}(\text{BN}(\text{Fc}(X))) \tag{1}$$

where X represents the model's input and Z represents the model's output. $X \in \mathbb{R}^{b\times d}$, $Z \in \mathbb{R}^{b\times d}$, where b denotes the batch size of EEG signal samples, and d denotes the feature dimension of the EEG signal samples.

Classifier The domain-specific classifiers use the features extracted by the domain-specific feature extractors to predict the results. In the domain-specific classifier, there are n separate softmax classifiers corresponding to the n source domains, and the final result is the average of the predictions from all classifiers. To train each classifier, we use the following cross-entropy loss to estimate the classification loss:

$$L_{cls} = \frac{1}{N_s}\sum_{i=1}^{N_s} y_s log(\widetilde{y}_s) \tag{2}$$

where N_s is the number of samples in the source domain, y_s is the true label, and $\widetilde{y}_s$ is the predicted label by the classifier.

Indirect Alignment Strategy

Mixed Source Domain In previous studies, there is no information transfer between individual source domains, which

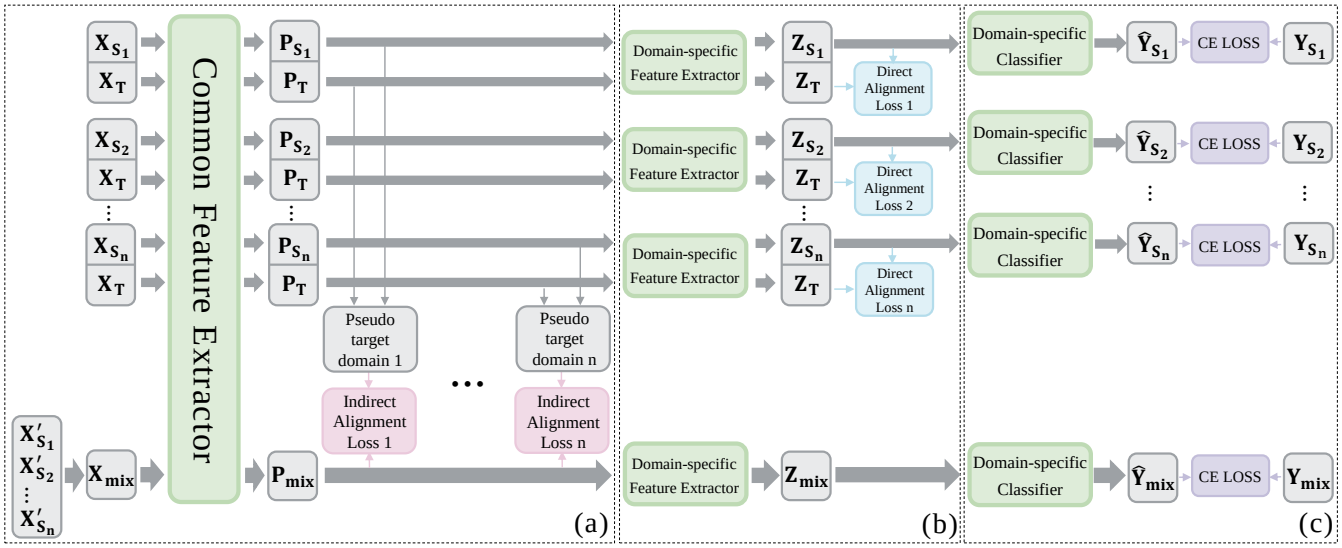

Figure 1: Overview of the JMS2A model architecture. Specifically, (a) the raw EEG signals are input into the shared feature extractor to obtain shallow common features, followed by the calculation of the indirect alignment loss. (b) The shallow common features are then passed to the domain-specific feature extractors to obtain deep discriminatory features, followed by the calculation of the direct alignment loss. (c) The deep discriminatory features are finally input into the domain-specific classifiers to generate predicted labels, and the predicted labels are compared with the true labels using cross-entropy loss to train the classifier's performance.

can result in large variance in the prediction results of the final n classifiers. To address this, we introduce the concept of a mixed source domain. Specifically, the data from all source domains are aggregated into one domain and shuffled, and samples from the mini-batch are randomly selected for subsequent processing during model training. Since the mixed source domain contains data from all source domains, the information it holds is more comprehensive than that of a single source domain. More importantly, it can transfer domain difference information between all source domains, thus indirectly accelerating the feature alignment process.

Pseudo Target Domain We combine the labeled source domain samples and the unlabeled target domain samples to form a pseudo-target domain. This approach is motivated by two key factors: First, domain differences exist not only between the source and target domains but also among the source domains themselves. By combining the source and target domains into a pseudo-target domain, we simulate a new, expanded target domain that helps reduce the domain differences among the source domains. Second, during model training, the two domains within the pseudo-target domain are mapped into the same feature space and brought closer together, which indirectly facilitates the alignment of features between the source and target domains.

Indirect Alignment Loss In the indirect alignment strategy, we explicitly match the feature distributions of the same class between the mixed source domain and the pseudo-target domain using the following formula:

$$L_{IA} = \sum_{k=1}^{K} dist(C_{ms}^{k}, C_{pt}^{k}) \tag{3}$$

where C_{ms}^{k} represents the centroid of the features of class k in the mixed source domain, and C_{pt}^{k} represents the centroid of the features of class k in the pseudo-target domain. The function $dist()$ measures the difference between the two centroids using cosine distance. $C_{ms}^{k} \in \mathbb{R}^{c \times d}$ and $C_{pt}^{k} \in \mathbb{R}^{c \times d}$, where c is the number of classes in the EEG signal samples and d is the feature dimension. Although the centroid helps suppress the impact of false pseudo-labels, to minimize the influence of pseudo labels, we use a moving average centroid here.

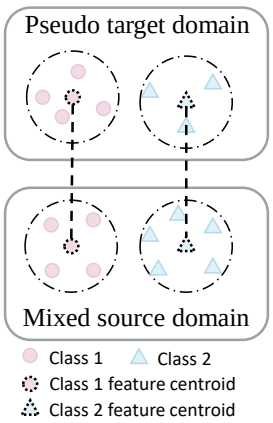

Figure 2: Illustration of the indirect alignment loss step.

The indirect alignment loss minimizes the distance between the centroids of the same class across different domains, facilitating the alignment of features belonging to the same class. The specific procedure is illustrated in Figure 2. First, we calculate the feature centroids for each class in both the mixed source domain and the pseudo-target domain. Then, we use cosine distance to measure the difference between the two domains. Finally, we reduce this difference to align the centroids of each class across the two domains. However, in unsupervised domain adaptation tasks, the labels of the target domain are unavailable. Therefore, we employ domain-specific classifiers to assign pseudo-labels to the pseudo-target domain samples, addressing the issue of missing label information.

Direct Alignment Strategy

Direct Alignment Loss In the direct alignment loss strategy, we extend the supervised contrastive learning loss to a semi-supervised contrastive learning form suitable for UDA. This extended loss can be seamlessly integrated into any UDA framework and enhances the adaptation of class discrimination knowledge. It brings features of samples belonging to the same class closer together, while pushing features of samples from different classes further apart. The definitions of supervised contrastive learning and the extended semi-supervised contrastive learning formula are as follows:

$$L_{DA}^{same} = \sum_{i \in I} \frac{-1}{|P(i)|} \sum_{p \in P(i)} log \frac{exp(z_i \bullet z_p)}{\sum_{a \in A(i)} exp(z_i \bullet z_a)} \tag{4}$$

$$L_{DA}^{diff} = \sum_{i \in I} \frac{-1}{|P(i)|} \sum_{q \in Q(i)} log \frac{exp(z_i \bullet z_q)}{\sum_{a \in A(i)} exp(z_i \bullet z_a)} \tag{5}$$

where I represents the set of all samples, and $A(i)$ represents the set of all samples except the i-th one, $P(i) = \{p \in A(i) : \widetilde{y}_p = \widetilde{y}_i\}$, $Q(i) = \{q \in A(i) : \widetilde{y}_q \neq \widetilde{y}_i\}$, and $\bullet$ denotes the dot product. z represents the simplified interaction features of the EEG signals. $z \in \mathbb{R}^{b \times d}$, where b is the batch size of EEG signal samples and d is the feature dimension of the EEG signal samples. Combining equations (5) and (6), the direct alignment loss function is defined as:

$$L_{DA} = L_{DA}^{same} - \lambda L_{DA}^{diff} \tag{6}$$

where λ is a hyperparameter.

Sample Pair Pseudo-label Acquisition Since the direct alignment loss relies on supervised contrastive learning, sample labels are essential. In UDA, target domain labels are unavailable, making the acquisition of pseudo-labels crucial. The quality of these pseudo-labels significantly influences the final performance of the direct alignment strategy. Instead of directly obtaining pseudo-labels for the target domain, we utilize simplified interactive features to capture the intrinsic relationships between different sample pairs. We then compute the pairwise similarity between samples to generate pseudo-labels for these sample pairs.

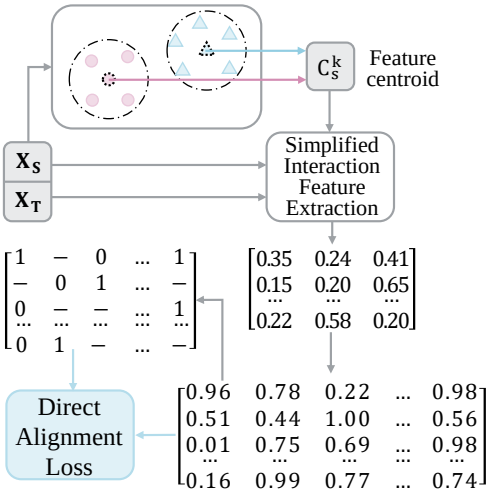

Figure 3: Illustration of the direct alignment loss step.

The specific operation is shown in Figure 3. First, we calculate the centroid of the sample features for each class in the source domain, which represents the mean of the sample features for that class. Next, we perform simplified interactive feature extraction by computing the dot product of all samples with the centroids of the source domain. This step produces feature representations that are more advantageous for the contrastive learning task. We then calculate the cosine similarity between all pairs of simplified interaction features. If the similarity is greater than 0.9, the pair is assigned a pseudo-label of 1 (indicating they belong to the same class), and the loss is computed using equation (4). If the similarity is less than 0.5, the pair is assigned a pseudo-label of 0 (indicating they belong to different classes), and the loss is computed using equation (5). Pairs with similarities between 0.5 and 0.9 are considered uncertain and are not assigned pseudo-labels. Our method does not directly acquire pseudo-labels for the samples; instead, it uses simplified interaction features to determine whether samples belong to the same class. This approach integrates the sample pair pseudo-labels with the direct alignment loss, reducing errors caused by pseudo-labels and enhancing the effectiveness of downstream direct alignment strategies.

Total Loss

We sum the previously mentioned cross-entropy loss, indirect alignment loss, and direct alignment loss to obtain the total loss, as follows:

$$L_{total} = L_{cls} + \alpha(\beta L_{IA} + L_{DA}) \tag{7}$$

here, α is calculated using the formula $\frac{2}{(1+e^{-10*\eta})} - 1$, where $\eta = \frac{iteration}{max\_iteration}$, with $iteration$ being the current iteration and $max\_iteration$ the total number of iterations. β is a hyperparameter that controls the model.

Experiments

Datasets

We conducted experiments on two publicly available EEG emotion datasets: SEED (Zheng & Lu, 2015) and SEED-IV (Zheng et al., 2018). The EEG data from both datasets were collected using a 62-channel ESI NeuroScan system, with electrode placements following the international 10-20 system.

SEED The SEED dataset consists of EEG emotion signals recorded from 15 subjects while watching 15 videos, which evoked three types of emotions: negative, neutral, and positive. The EEG data includes recordings from three different time periods, approximately once a week, corresponding to three sessions.

SEED-IV The SEED-IV dataset consists of EEG emotion signals recorded from 15 subjects while watching 24 videos, which evoked four types of emotions: happiness, sadness, fear, and neutral. Like the SEED dataset, the EEG data includes recordings from three different time periods, approximately once a week, corresponding to three sessions.

Data Processing We directly used the pre-computed differential entropy features provided by the SEED and SEED-IV datasets (Y. Wang et al., 2021; Zheng et al., 2018). The raw EEG signals from both datasets were downsampled to 200 Hz and then band-pass filtered in the range of 1-75 Hz. The filtered signals were subsequently segmented into 1-second and 4-second segments. For SEED, since the length of each EEG trial varied, we trimmed each trial signal to a consistent length and processed them using a 9-second window with 8-second overlap (L. Yang & Liu, 2019). For SEED-IV, no special processing was applied. Finally, for both datasets, Z-score normalization was performed on the processed EEG data for each subject in each session by subtracting the mean and dividing by the standard deviation.

Implementation Details

In our experiments, we used leave-one-subject cross-validation to evaluate the performance of the proposed method in the cross-subject task. During the cross-validation process, no information leakage occurs between the source and target domain data, as they are from different subjects. It is worth noting that, unlike the approach of Zhang et al. (2024), our method exclusively uses target domain data during model training and does not involve any label information. We set the mini-batch size for all domains to 50, as variations in batch size do not significantly affect model performance. Additionally, we employed the RMSprop optimizer for model training, with a learning rate of 1e-3 and an L2 regularization weight factor of 1e-5. The SEED dataset was trained for 2000 iterations, while the SEED-IV dataset was trained for 3000 iterations. For the SEED task, we set λ and β to 0.01 and 1, respectively; for the SEED-IV task, λ and β were set to 1 and 0.01, respectively.

Our model was trained on an NVIDIA GeForce GTX 3060 12GB GPU using Windows 11 22H2, PyTorch 1.12.1, Python 3.10.13, and CUDA 11.3.

Results

We compared the proposed JMS2A model with state-of-the-art methods, as presented in Tables 1 and 2. MS-MDA (Chen et al., 2021) simultaneously considers both the domain invariance and domain specificity of EEG signals, enabling the extracted features to undergo finer-grained domain alignment. MFA-LR (Jiménez-Guarneros & Fuentes-Pineda, 2023) and Gusa (X. Li et al., 2024) build on MFA-LR by incorporating pseudo-label correction strategies and multi-level graph convolution modules, respectively. The former fully leverages target domain label information, making the model more robust, while the latter exploits the spatial structure of EEG channels to improve model recognition capability. Moreover, (Zhou et al., 2023) is the first to introduce prototype learning into EEG emotion recognition, transforming the emotion recognition task into pairwise learning to improve the model's tolerance to noisy labels. S2A2-MSDA (Y. Yang et al., 2024) proposes a spectral-spatial attention mechanism to learn rich domain-invariant features, enabling the model to easily generalize to new subjects. Our proposed model achieved accuracies of 95.30%, 92.02%, and 91.24% across three sessions on the SEED dataset, and 80.79%, 86.55%, and 82.48% across three sessions on the SEED-IV dataset.

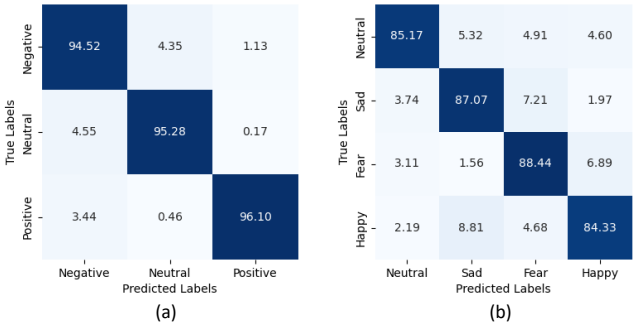

Figure 4: Confusion matrix for JMS2A. Each row represents the true class and each column represents the predicted class of the model output. (a) Confusion matrix for SEED. (b) Confusion matrix for SEED-IV.

Figure 4 shows the confusion matrix for the best session of the JMS2A model on two datasets. Each row represents the true class, while each column corresponds to the predicted class output by the model. The color intensity indicates the accuracy. On the SEED dataset, our model performs better in identifying negative emotions than in recognizing positive and neutral emotions, suggesting that the model better leverages information from negative emotions. On the SEED-IV dataset, the model achieves relatively high accuracy in identifying fear, while the accuracy for happy emotions is lower, indicating that non-happy emotions are more easily recognized.

Table 1: The comparison of accuracy performance (%) of different studies on the SEED dataset.

Method	Session 1	Session 2	Session 3	Best Session	Average
MS-MDA	85.65 ± 05.37	85.32 ± 07.97	85.12 ± 09.46	85.65 ± 05.37	85.36
S2A2-MSDA	90.11 ± 07.32	/	/	/	/
MFA-LR	89.73 ± 06.98	83.16 ± 12.91	84.93 ± 11.58	89.73 ± 06.98	85.94
PR-PL	93.06 ± 05.12	88.38 ± 07.85	87.01 ± 09.37	93.06 ± 05.12	89.48
Gusa	91.77 ± 05.91	/	/	/	/
Ours	**95.30 ± 04.17**	**92.02 ± 07.12**	**91.24 ± 07.83**	**95.30 ± 04.17**	**92.85**

Table 2: The comparison of accuracy performance (%) of different studies on the SEED-IV dataset.

Method	Session 1	Session 2	Session 3	Best Session	Average
MS-MDA	67.06 ± 09.61	72.38 ± 08.88	68.40 ± 12.24	72.38 ± 08.88	69.28
S2A2-MSDA	/	/	/	/	76.23
MFA-LR	66.35 ± 14.02	77.05 ± 13.45	70.31 ± 15.25	77.05 ± 13.45	71.23
PR-PL	71.05 ± 07.97	81.32 ± 08.53	74.32 ± 15.13	81.32 ± 08.53	75.53
Gusa	/	/	/	/	75.12
Ours	**80.79 ± 08.24**	**86.55±06.94**	**80.09 ± 11.11**	**86.55±06.94**	**82.48**

Table 3: Ablation study on the SEED and SEED-IV datasets.

Method	SEED	SEED-IV
w/o direct alignment loss (diff)	94.71	82.35
w/o direct alignment loss(all)	89.67	81.54
w/o indirect alignment loss	93.32	82.87
w/o mixed source domain	93.40	84.09
— w/o direct alignment loss (diff)	92.58	80.84
— w/o direct alignment loss (all)	89.08	80.22
Ours	95.30	86.55

Ablation Study

We conducted ablation experiments on the SEED and SEED-IV datasets to validate the effectiveness of each module in the proposed model. The results are shown in Table 3.

(1)Removing the semi-supervised loss term from the direct alignment loss: After removing this term, the model loses some of the potential class information from the target domain. As a result, the accuracy on SEED and SEED-IV decreased by 0.59% and 4.2%, respectively.

(2)Removing the entire direct alignment loss: Without the entire direct alignment loss, the model no longer extracts potential class information from the target domain, leading to a decrease in accuracy by 5.63% on SEED and 5.01% on SEED-IV.

(3)Removing the indirect alignment loss: Ignoring the structured information from the source domain results in a decrease in accuracy by 1.98% on SEED and 3.68% on SEED-IV.

(4)Removing the mixed source domain: Additionally, we examined the effect of removing both the semi-supervised loss term and the entire direct alignment loss after removing the mixed source domain. As presented in Table 3, the mixed source domain plays a crucial role in transferring source domain information, thereby facilitating feature alignment.

In summary, every module in the model is meaningful and effective, contributing significantly to the improvement of the model's performance.

Conclusion

In this paper, we propose an unsupervised domain adaptive model with joint multi-source domain and two-step alignment strategy (JMS2A). This model is capable of extracting and leveraging the structured information from the source domain data, as well as the latent class information from the target domain data. We construct public feature extractors for extracting shallow public features and domain-specific feature extractors for extracting deep differential features in this model. In addition, we incorporate a two-step alignment strategy into the model. The first step involves indirectly aligning the mixed source and pseudo-target domains, while the second step focuses on directly aligning the source and target domains. The experimental results demonstrate that our model outperforms existing methods in cross-subject classification tasks, and the effectiveness and significant contribution of each module to these tasks are validated through ablation experiments. However, our model currently incurs significant computational overhead during the training process. In the future, we plan to improve the network architecture, adopt more efficient training strategies, and enhance the model's computational efficiency.

Acknowledgments

This work was supported by the Natural Science Foundation of China (62374121,61974109).

References

Chen, H., Jin, M., Li, Z., Fan, C., Li, J., & He, H. (2021). Ms-mda: Multisource marginal distribution adaptation for cross-subject and cross-session eeg emotion recognition. *Frontiers in Neuroscience*, *15*, 778488.

Ekman, P. (1993). Facial expression and emotion. *American psychologist*, *48*(4), 384.

Ioffe, S. (2015). Batch normalization: Accelerating deep network training by reducing internal covariate shift. *arXiv preprint arXiv:1502.03167*.

Jiménez-Guarneros, M., & Fuentes-Pineda, G. (2023). Learning a robust unified domain adaptation framework for cross-subject eeg-based emotion recognition. *Biomedical Signal Processing and Control*, *86*, 105138.

Jin, Y.-M., Luo, Y.-D., Zheng, W.-L., & Lu, B.-L. (2017). Eeg-based emotion recognition using domain adaptation network. In *2017 international conference on orange technologies (icot)* (pp. 222–225).

Li, X., Chen, C. P., Chen, B., & Zhang, T. (2024). Gusa: Graph-based unsupervised subdomain adaptation for cross-subject eeg emotion recognition. *IEEE Transactions on Affective Computing*.

Li, Y., Zheng, W., Zong, Y., Cui, Z., Zhang, T., & Zhou, X. (2018). A bi-hemisphere domain adversarial neural network model for eeg emotion recognition. *IEEE Transactions on Affective Computing*, *12*(2), 494–504.

Lotte, F., Bougrain, L., Cichocki, A., Clerc, M., Congedo, M., Rakotomamonjy, A., & Yger, F. (2018). A review of classification algorithms for eeg-based brain–computer interfaces: a 10 year update. *Journal of neural engineering*, *15*(3), 031005.

Paranjape, R., Mahovsky, J., Benedicenti, L., & Koles, Z. (2001). The electroencephalogram as a biometric. In *Canadian conference on electrical and computer engineering 2001. conference proceedings (cat. no. 01th8555)* (Vol. 2, pp. 1363–1366).

Saha, P., Fels, S., & Abdul-Mageed, M. (2019). Deep learning the eeg manifold for phonological categorization from active thoughts. In *Icassp 2019-2019 ieee international conference on acoustics, speech and signal processing (icassp)* (pp. 2762–2766).

Tyng, C. M., Amin, H. U., Saad, M. N., & Malik, A. S. (2017). The influences of emotion on learning and memory. *Frontiers in psychology*, *8*, 235933.

Wang, F., Zhang, W., Xu, Z., Ping, J., & Chu, H. (2021). A deep multi-source adaptation transfer network for cross-subject electroencephalogram emotion recognition. *Neural Computing and Applications*, *33*, 9061–9073.

Wang, M., & Deng, W. (2018). Deep visual domain adaptation: A survey. *Neurocomputing*, *312*, 135–153.

Wang, Y., Qiu, S., Ma, X., & He, H. (2021). A prototype-based spd matrix network for domain adaptation eeg emotion recognition. *Pattern Recognition*, *110*, 107626.

Xu, Y., Du, Y., Li, L., Lai, H., Zou, J., Zhou, T., ... Ma, P. (2023). Amdet: Attention based multiple dimensions eeg transformer for emotion recognition. *IEEE Transactions on Affective Computing*.

Yang, L., & Liu, J. (2019). Eeg-based emotion recognition using temporal convolutional network. In *2019 ieee 8th data driven control and learning systems conference (ddcls)* (pp. 437–442).

Yang, Y., Wang, Z., Tao, W., Liu, X., Jia, Z., Wang, B., & Wan, F. (2024). Spectral-spatial attention alignment for multi-source domain adaptation in eeg-based emotion recognition. *IEEE Transactions on Affective Computing*.

Zhang, Q., Yang, L., et al. (2024). Cross-subject emotion classification based on dual-attention mechanism and meta-transfer learning. In *Proceedings of the annual meeting of the cognitive science society* (Vol. 46).

Zheng, W.-L., Liu, W., Lu, Y., Lu, B.-L., & Cichocki, A. (2018). Emotionmeter: A multimodal framework for recognizing human emotions. *IEEE transactions on cybernetics*, *49*(3), 1110–1122.

Zheng, W.-L., & Lu, B.-L. (2015). Investigating critical frequency bands and channels for eeg-based emotion recognition with deep neural networks. *IEEE Transactions on autonomous mental development*, *7*(3), 162–175.

Zhou, R., Zhang, Z., Fu, H., Zhang, L., Li, L., Huang, G., ... others (2023). Pr-pl: A novel prototypical representation based pairwise learning framework for emotion recognition using eeg signals. *IEEE Transactions on Affective Computing*, *15*(2), 657–670.